Quince seed mucilage-based scaffold as a biocompatible engineered substrate to promote fibroblasts proliferation, human adipose-derived stem cells differentiation into keratinocytes and skin regeneration

Azadeh Izadyari Aghmiuni[1,6*], Saeed Heidari Keshel[2,3*], Farshid Sefat[4,5], Azim Akbarzadeh Khiyavi[6]

[1] Department of Chemical Engineering, Ayatollah Amoli Branch, Islamic Azad University, Amol, Iran.
[2] Medical Nanotechnology Research Center, Shahid Beheshti University of Medical Sciences, Tehran, Iran.
[3] Department of Tissue Engineering and Applied Cell Science, School of Advanced Technologies in Medicine, Shahid Beheshti University of Medical Sciences, Tehran, Iran.
[4] Department of Biomedical and Electronics Engineering, School of Engineering, University of Bradford, Bradford, UK.
[5] Interdisciplinary Research Centre in Polymer Science & Technology (IRC Polymer), University of Bradford, Bradford, UK.
[6] Department of Nanobiotechnology, Pasteur Institute of Iran, Tehran, Iran.

***Corresponding Author Email:** azadeh.izadyari@gmail.com**;** saeedhey@gmail.com

Abstract

The use of bioactive materials like quince seed mucilage (QSM), as the common curative practice has a long history in Iranian traditional medicine to cure wounds and burns. However, this gel cannot be applied on exudative wounds. It also limits cell-to-cell interactions and lead to the slow wound healing process. The design of bioactive materials-based 3D scaffolds may be effective in overcoming the mentioned problems and increasing their therapeutic capacities. To this end, a novel QSM-based hybrid scaffold modified by PCL/PEG copolymer was designed and characterized using physicochemical and biological experiments (FTIR, tensile, SEM, swelling, cell adhesion, proliferation, gene expression). The properties of this scaffold (PCL/QSM/PEG) were also compared with four scaffolds of PCL/PEG, PCL/Chitosan/PEG, chitosan, and QSM, to assess the role of various materials and the combined effect of polymers in improving the function of skin tissue-engineered scaffolds. It was found, the physicochemical properties play a crucial role in regulating cell behaviors (survival, growth, keratinocytes differentiation of human adipose-derived stem cells (h-ASCs)). Comparison of results indicated, PCL/QSM/PEG scaffold as a smart/stimuli-responsive biomatrix promotes not only h-ASCs adhesion but also supports human skin fibroblasts growth, via providing a porous-network with the appropriate pores size for the growth of skin cells. PCL/QSM/PEG could also induce epidermal/dermal keratinocytes at a desirable level for wound healing, by increasing the mechanical signals transduction to the biological signals. Immunocytochemistry analysis confirmed keratinocytes differentiation pattern (in the early and late phases) and their normal phenotype (polygonal shape) on PCL/QSM/PEG. Our study demonstrates that PCL/QSM/PEG scaffold as a differentiation/growth-promoting factor can be a proper candidate for the design of wound dressings and skin-engineered substrates containing cell.

Keywords: Bioactive materials, Quince seed mucilage, 3D scaffolds, Skin cells differentiation, Wound dressing.

Introduction

The skin is known as the largest organ in the body which comprises three layers of the epidermis (consists of complex cell-cell interactions), dermis (consists of follicles, glands, nerves, and capillary vessels are embedded), and the hypodermis (consists of blood vessels and adipose tissue) [1–3]. This tissue plays a crucial role in the physical protection of internal organs and the prevention and control of infectious and bacteria in the body [2,4]. Hence, any damage (mechanical or chemical) to the skin layers require immediate treatment. In this field, the xenografts, allografts, and autografts were the main treatment in past decades, but ethical constraints and lack of donor sites enforced were led to a decrease in the use of these methods [5–7]. Nowadays, skin tissue-engineered substrates have rapidly developed as an alternative method for wound healing [6]. The various studies have shown that an ideal skin-engineered scaffold should promote not only dermal fibroblast cells proliferation, but also should express dermal and epidermal keratinocytes induced by stem cells differentiation [3,8,9]. Such a scaffold as a skin substitute can be effective in the treatment of large wounds and stimulation of skin regeneration [3,9,10]. Although, many attempts have been made in this field, however, the main challenge in skin tissue engineering is the design of a dermal ECM[1]-like scaffold that can mimic the structure and biomechanical and physicochemical functions of the normal skin to better proliferate and differentiate stem cells into the epidermis or dermis cells.

In this field, hyaluronic acid and chitosan (natural polysaccharides), as well as poly (ε-caprolactone) (PCL) and polyethylene glycol (PEG) (synthetic polymers) are the most famous materials that are widely applied in the structure of dermal substitutes [11–15]. These polymers play a crucial impact on the cell function and mechanical strength of scaffold via the creation of integrity chemical structure [16–18]. However, there is no material that fully remodels the ECM network and simulates the biological behavior of the skin. Therefore, the studies have still continued to achieve ideal skin scaffolds with proper biological approaches.

Although, some of the reports have indicated that bioactive materials/molecules like herbal extracts or oil/mucilage extracted from fruits seed can regenerate dermal-ECM and accelerate the wound healing process [19–25]. Common applications of these bioactive materials include ointments, creams or hydrogel formulations that can be used directly on the surface of the dried wounds [26–30]. It is notable that, the disadvantages of the use of bioactive materials in the mentioned forms are their inability to absorb wound exudates and maintain a stable shape on the wound surface [31]. Additionally, such products should not be applied to open wounds due to the probability of the spread of infection in the wound area [31].

However, it seems that the bioactive materials due to their multiple-properties such as antibacterial, cell proliferation, biodegradability, and biocompatibility can be used as a proper alternative for natural polymers in the structure of skin tissue engineered scaffolds or act as growth factors for induction of keratinocytes, fibroblasts proliferation and wound healing, in vitro and in vivo [25,31,32]. Nevertheless, there were few studies that have evaluated the stem

[1] Extra Cellular Matrix

cells differentiation effects on the bioactive materials-based scaffolds for induction of particular cells [33].

Given the above cases, polymers blending can be one of the most effective methods for the design of ideal scaffolds or wound dressings in skin tissue engineering applications to accelerate wound healing [8,34]. In this field, selection of bioactive material can also play an important role in cell proliferation/differentiation and skin regeneration.

Quince-seed is one of these therapeutic bioactive-materials that has widely used in Iranian traditional medicine for the reduction of pain and inflammation, the wound healing and re-epithelialization of skin (scar-free) [20,32,35]. Although phytochemical researches confirm therapeutic and regenerative effects of this bioactive material, however, the physical form of this gel cannot be applied on exudative wounds and rapidly will dry up in the open-air if it is not covered, because of the high water content. Furthermore, this gel might limit cell-to-cell interactions due to limitations in providing sufficient pores within its structures that can lead to a slow wound healing process.

In order to overcome the mentioned problems and achieve a desirable substrate, a novel quince seed mucilage-based 3D scaffold modified by PCL/PEG copolymer was here designed that can remodel not only 3D-network of ECM but also mimic its physicochemical and biological functions to accelerate wound healing process. The PCL/PEG, PCL/chitosan/PEG, chitosan and quince seed mucilage (QSM) scaffolds were also fabricated to study the role of QSM and the combined effect of bioactive materials, natural and synthetic polymers on cellular functions, swelling index and wound exudates absorption capacity. In followed by, the physicochemical and mechanical properties of scaffolds were evaluated to understand cells signaling and how to induce the cells and treat the dermal wounds. Afterward, the efficiency of the scaffolds in promoting the growth of human dermal fibroblasts, as well as increasing the cell attachment, proliferation, and differentiation of human adipose stem cells (h-ASCs) into both keratinocytes of epidermal and dermal was evaluated by scanning electron microscope imaging, gene expression analysis and immunocytochemistry assay. It is notable that h-ASCs were selected because of ease of isolation and ethical considerations (lower concerns in conducting research) [36,37]. Moreover, the freeze-drying technique as an affordable method utilized for preparing the 3D porous scaffolds.

2. Materials and methods

2.1. Materials

Quince fruits (*Cydonia oblonga*) were purchased from a garden in the city of Isfahan, Iran (early fall). Moreover, the medical grade chitosan (95% deacetylation, an average molecular weight of 234 kDa), poly-ε-caprolactone (Mn: 45000), polyethylene glycol (Mn: 6000), N-hydroxysuccinimide (NHS), 1-Ethyl-3-[3-dimethylaminopropyl]carbodiimide hydrochloride (EDC), glacial acetic acid, tetrazolium salt 3-(4, 5-dimethylthiazol- 2-yl)-2,5-diphenyltetrazolium bromide (MTT) and dimethyl sulfoxide (DMSO), and lysozyme were purchased from Sigma (USA). Dulbecco's modified eagle's medium-low glucose (DMEM-

LG), fetal bovine serum (FBS), bovine serum albumin (BSA), penicillin-streptomycin were also obtained from Gibco (USA). Human skin fibroblast cells line (HSF, NCBI Code: C192) were provided by Iranian Pasture Institute cell bank, Tehran, Iran.

2.2. Copolymer solutions preparation

To prepare quince seed mucilage (QSM) with the weight fraction of 5 wt%[2] and appearance of a viscous gel, quince-seeds were separated from the pulp and dried under shade for 2-3 weeks. Then, 5g of dried seeds were macerated in 10 mL of dH_2O[3], for 24 h. Furthermore, the poly-ε-caprolactone (PCL) and polyethylene glycol (PEG) solutions with the weight fractions of 3 and 10 wt% were obtained by dissolving the calculated amount of PCL and PEG powder in 70% acetic acid (40° C) and dH_2O (25° C) respectively, for 24 h. Similarly, the chitosan solution (5 wt%, in 0.05 M[4] acetic acid) was prepared at 25° C, for 24 h.

2.3. Fabrication of porous scaffolds

The solutions of PCL/PEG (PCPE), PEG-QSM-PCL (PQP) and PEG-Chitosan-PCL (PCP) were prepared at a ratio of 1:1.5 and 1.5:2:1 (v/v)[5] respectively, and stirred for an additional 24 h. It is notable that the NHS/EDC crosslinking solution in a volume ratio of 1:5 v/v was added to mixed solutions (10% of total solution volume) to improve interactions between polymer chains. Afterward, 2 mL of each solution were cast into 24-well plates (Sigma, USA) and frozen at -20°C and -80°C respectively, for 48 h. In followed by, frozen solutions were dried by freeze-drying for 72 h to prepare the porous scaffolds.

The QSM and chitosan solutions were also lyophilized in the same manner to evaluate the chemical structures and interactions between polymer chains. Finally, all the scaffolds were stored at 4°C.

2.4. Physiochemical characterizations of scaffolds

2.4.1. Surface chemistry study (FTIR[6]): To characterize the polymers interactions and surfaces chemistry, the lyophilized scaffolds were evaluated by FTIR-spectrum analysis (Model-ALPHA, Bruker, Germany). The spectra of scaffolds were recorded in the range of 400–4000 cm-1 with 4 cm-1 resolution and an average of 16 scans.

2.4.2. Degradation profile and swelling percentage: In vitro degradation rate of scaffolds was evaluated by monitoring the mass remaining. In brief, the weight of scaffolds were recorded before putting in culture medium containing 13 mg/L lysozyme, then immersed in medium and incubated in 37°C for 2, 4, 8, and 14 days. At the end of each period, the scaffolds were taken out of the medium, washed thoroughly with dH_2O, and weighed after dried by freeze-drying (4 h). The degradation percentage and mass remaining of scaffolds were obtained according to equation (1) [38].

[2] Percent by weight Fraction or percent of solute in the solution is given the symbol w/w % or (wt %).
[3] Deionized water
[4] Molarity (M) is the concentration of a solution expressed as the number of moles of solute per liter of solution.
[5] Volume ratio (vol/vol or v/v)
[6] Fourier Transform Infrared Spectroscopy

In followed by, to determine the swelling percentage, scaffolds with a known weight were soaked into phosphate-buffered saline (PBS, pH= 5.5). After 1 and 24 h, the excess PBS was removed and the scaffolds were weighted again. Finally, the percentage of scaffolds swelling was calculated through equation (2) [39]. Three scaffolds for each group were used to measure the average value of degradation % and swelling % along with their standard deviations (SD).

$$\begin{cases} \text{Degradation \%} = \dfrac{W_d - W_t}{W_d} \times 100 \\ \text{Mass remaining \%} = 100 - \text{Degradation \%} \end{cases} \quad \text{(Eq. 1)}$$

$$\text{Swelling \%} = \frac{W'_t - W'_d}{W'_d} \times 100 \quad \text{(Eq. 2)}$$

Here, (W_d) and (W_t) are the weight of the scaffolds before and after degradation [at the time (t)], respectively. Moreover, (W'_d) and (W'_t) are initial dry weight and weight of the swollen scaffold at hours 1 and 24.

2.4.3. Mechanical behavior: To determine the mechanical properties of the scaffolds (10×5×2 mm^3), a tensile test was carried out using a tensile tester instrument (Zwick/Roell, 1446, Germany), at a strain rate of 2 mm/min, and the ASTM D3039 standard guide for testing polymer matrix composite materials [40]. Five samples (n=5) were tested for each scaffold and values expressed as mean ± SD.

2.4.4. Scaffolds porosity (%): The porosity of the scaffolds was measured by a liquid displacement method [41]. Briefly, scaffolds with a known weight (W_d) were immersed in absolute ethanol (25°C, 1 h), then taken out and reweighed (W_w). The porosity was determined with equation (3). Three scaffolds (n=3) for each group were used to measure the average value along with SD.

$$\text{Porosity \%} = \frac{W_w - W_d}{\rho \times \upsilon} \times 100 \quad \text{(Eq. 3)}$$

The ρ and υ are the density of ethanol and the volume of the swollen scaffolds, respectively.

2.4.5. Morphology analysis: The morphology of porous scaffolds were analyzed using a scanning electron microscope (SEM, XL30 ESEM, Philips, Germany), at an accelerating voltage of 20 kV. Prior to SEM analysis, the surface of the scaffolds was coated with thin layer of Au (gold) and their morphology and pores diameter were evaluated by Clemex vision software 3.5 by choosing 50 locations on the surfaces randomly. The values were expressed as the mean ± SD, n = 3.

2.5. Biological behavior on the scaffolds

The study of cell behavior (adhesion, viability, and proliferation) was performed to test scaffolds biocompatibility and biological efficiency. The 3rd passage of human eyelid adipose-derived stem cells (h-ASCs) isolated in our previous study was used in this research [42]. Prior

to cell seeding, scaffolds were immersed in 75% alcohol (1 h), washed two times with a solution of PBS, and sterilized by ultraviolet (UV rays, 254 nm wavelength, 2 h), then placed into 24-well plates.

Afterward, the suspended h-ASCs in the culture medium containing DMEM-low glucose, 15% FBS, and penicillin (100 U/mL)/streptomycin (1000 U/mL), at a density of 1×10^6 cells/well were seeded onto the porous scaffolds.

After 5 h of incubation at 37° C, 5% CO_2 and humidified atmosphere, scaffolds containing cell were observed under SEM to evaluate initial adhesion (cell/scaffold interactions) and distribution of h-ASCs on the scaffolds. Briefly, the culture medium was removed and scaffolds were washed with PBS, then cells were fixed with 3% glutaraldehyde solution. After 30 min, the scaffolds were washed again with PBS and post-fixation was performed with 1% Osmium tetroxide. Finally, the cell/scaffold constructs were observed under SEM at an accelerating voltage of 10.0 kV.

An MTT assay was also carried out to assess the h-ASCs viability on the scaffolds. In brief, after 24, 48 and 72 h of culture, the medium of each well was removed and replaced with 100µl of fresh medium and 20µl of MTT solution. After incubation for 4 h, MTT medium was removed, and cells were solubilized in 100µl of DMSO. Then, the absorbance of each sample at a wavelength of 570 nm was determined with an ultraviolet-visible spectrophotometer (Shimadzu UV-1601, Kyoto, Japan). The culture medium (without scaffolds) was selected as the control group (100% cell viability). The cell viability (%) was estimated by equation (4) [43]. It is notable that all values were expressed as mean ± SD, n = 3.

$$\text{Cell viability (\%)}=\frac{OD_{sample}}{OD_{control}}\times100 \qquad \text{(Eq. 4)}$$

Furthermore, the proliferation of h-ASCs and human skin fibroblast (HSF) cell line (1×10^6 cells/well) on the scaffolds was separately determined by the observation of cell/scaffold constructs under the inverted microscope (Nikon Corporation, Tokyo, Japan) to evaluate the biological efficiency of the porous scaffolds in skin tissue engineering applications as a differentiation substrate or wound dressing. To this end, the cell/scaffold constructs were collected at day 3 of the cell culture and observed by the inverted microscope with a 20x magnification.

2.6. Gene expression analysis by Real-Time PCR[7]

The analysis of RT-PCR was carried out to assess the expression of keratinocyte-specific genes at days 7 and 14 of the h-ASCs differentiation, according to the standard protocol [44]. RNA extraction kit (Fermentas International, Burlington, Canada) was used for isolation of total RNA from cells placed on the scaffolds. Followed by, for digestion and removal of

[7] Polymerase chain reaction (PCR)

genomic DNA from extracted RNA, a DNase I treatment (Fermentas International, Burlington, Canada) was performed and the quantity of isolated RNA was evaluated using spectrophotometry (NanoDrop; Thermo, Wilmington, USA). Moreover, standard reverse transcription (RT) reactions were performed with 2 µg total RNA using RevertAid First Strand cDNA Synthesis Kit (Fermentas International, Burlington, Canada). Extracted RNA from the human normal skin cell line (C192, Iranian Pasture Institute cell bank) was also applied as a positive control.

The RT-PCR (Rotor-Gene Q Real-Time PCR System, Qiagen, USA) reaction was carried out with SYBRR Premix Ex Taq™ (Takara BIO, INK, Japan) that uses Taq Fast DNA Polymerase, SYBR Green I dye to detect double-stranded DNA.
The gene expression levels were obtained using the $2^{-\Delta\Delta Ct}$ method (normalized against human β-actin (ACTB) as a housekeeping gene) and statistical analysis were performed using ANOVA (p-value< 0.05). The gene-specific primers were used as below: keratinocyte10 (keratin10 or K10) (NM000421.3), forward: 5′-ACTACTCTTCCTCCCGCAGT and reverse: 5′-CAGAGCTCCCACGGCTAAAA (T_m: 60°C); K14 (NM000526.4), forward: 5′-AGACCAAAGGTCGCTACTGC and reverse: 5′-ATCGTGCACATCCATGACCT (T_m: 60°C); K18 (NM_000224.2), forward: 5′-AAGCCTGAGTCCTGTCCTTTCT and reverse: 5′-AGGCTTTGCATGGTCTCCTT (T_m: 61°C), as well as β-actin (ACTB) (NM001101.4), forward: 5′-GGCGCCCTATAAAACCCAGC and reverse: 5′-GCTCGATGGGGTACTTCAGG (T_m: 60°C).

2.7. Immunocytochemistry (ICC) assay

To direct immunocytochemistry (ICC) assay, at days 7 and 14 of co-culturing process, h-ASCs cultured on the sterilized scaffolds were washed with PBS (three times). In followed by, endogenous peroxidase activity was inactivated by 3% hydrogen peroxide (H_2O_2) solution according to the standard protocols. Afterward, plates were incubated in a blocking solution containing 1% BSA at 25 C for 1 h, to block non-specific sites. The scaffolds were then incubated at 4° C (overnight) with primary antibodies namely Anti-Cytokeratin 10 antibody [RKSE60] (ab9025), Anti-Cytokeratin 14 antibody [LL002] (ab7800) and Anti-Cytokeratin 18 antibody [C-04] (ab668); Abcam. After being labeled with primary antibody, the h-ASCs on the scaffolds were incubated with FITC-conjugated anti-rabbit IgG (BD Pharmingen™) as secondary antibody, for 2 h at room temperature. After rinsing the scaffolds with PBS, immunoreactive cells were visualized by fluorescent microscopy (LabPro CETI, Oxford).

2.7. Statistical analysis

Statistical analysis was performed by using the one-way analysis of variance (ANOVA) with Dunnett's (2-sided) and LSD's post hoc test IBM SPSS Statistics 24 and Graph Pad Prism 6 Demo software. P-values of <0.05, <0.01 and < 0.001 were considered as the significance levels. The results were expressed as mean ± standard deviation, n= 3, 5.

3. Results and discussion

The mucilage or gel extracted from fruits seed as a potential bioactive-material has a long history of curative properties in burns and wounds healing. In this field, the quince seed mucilage (QSM) has widely used in Iranian traditional medicine for creating new extra cellular matrix, wound healing, and skin regeneration [20,32,35]. These properties are related to biocompatible polysaccharide components of glucuronic acid and xylose (glucuronoxylan) which is extruded from the quince seeds [45]. Experimental and clinical studies have been approved benefits of this viscous gel for skin wounds healing [32,35].

The QSM possesses high water absorption capacity and can regulate the moisture level of the dried wounds for the re-epithelialization. However, this feature can lead to wound dryness if wound area is not covered. Lack of sufficient pores within the quince-seed gel matrix (due to saturation of gel by water, which provides an impermeable nature for the matrix) can also lead to a limitation in cell-cell signaling and consequently slow wound healing process. Further, extracted mucilage from quince-seed cannot be used on exudative wounds and open wounds because of its impermeable nature and the probability of growth of bacteria, and the spread of infection in the wound. It is notable that QSM storage is also difficult for a long time because of the growth of mold in the gel.

To overcome the mentioned problems, for the first time, we designed a novel hybrid 3D scaffold of QSM modified by PCL/PEG copolymer. The mentioned 3D scaffold fabricated using freeze-drying method to increase scaffold porosity and improve cellular function. The present study also was to assess the role of QSM (as an alternative bioactive material for natural polymers like chitosan) in the improvement of engineered scaffolds/dressings properties for in vivo skin tissue regeneration approaches, as well as to investigate the potential of cell adhesion, fibroblast proliferation and keratinocytes differentiation of h-ASCs on the bioactive material-based scaffolds and consequently acceleration of wound healing, in absence of growth factors. For this end, the physicochemical and biological properties of scaffolds were studied and compared, because these characteristics play an important role in understanding of biological behavior of scaffold, cell-scaffold interactions (cell responses), and how to mimic the growth pattern of the cell for supporting and guiding new tissue on the scaffold, in vivo applications of skin regeneration [46–48].

3.1. Surface chemistry analysis

The surface chemical analysis of the 3D porous scaffolds was carried out using FTIR spectrometer. Fig. 1A shows the FTIR spectra of the scaffolds. The absorption bands at 3000-3500 cm^{-1} are related to N-H stretch of primary amine/amide groups, and terminal -OH (hydroxyl) groups. In this region, the PQSP scaffold showed a stronger peak compared to other scaffolds that could be due to the formation of stronger intermolecular forces between QSM and synthetic polymers, and/or more hydrophilic groups in the PQSP structure.

All the peaks at 2865-2960 cm^{-1} are attributed to C-H band. Although the mentioned absorption band for PQSP appeared at a lower intensity relative to other scaffolds that can be explained

by better interactions of polymer chains. Similarly, the intensity of the peak in the region of 1700-1730 cm^{-1} that assigned to the ester carbonyl (in PCL) and amide I groups (in chitosan and QSM) was reduced in the PQSP spectrum, due to the interaction between ester carbonyl and amide groups. Furthermore, the existence of a peak at 1630-1645 cm^{-1} is related to C-O stretching and C-H bending bands of amide I and the primary amine, respectively *(*light green region) that can improve biological function of scaffold. It is notable that, the range and intensity changes of the peaks are related to how the functional groups to participate in chemical reactions and formation of new bonds [49]. Overall, the spectrum of QSM is similar to chitosan and hence, it can be predicted that both scaffolds will show similar physical, mechanical and biological properties, in vitro.

However, the comparison of spectra indicated that the QSM significantly changes when combined with PCPE copolymer, while no major difference in the main peaks of spectra was observed between chitosan and PCP scaffolds. It can be attributed to functional groups activity of QSM and the formation of a large number of intermolecular forces in the PQSP structure.

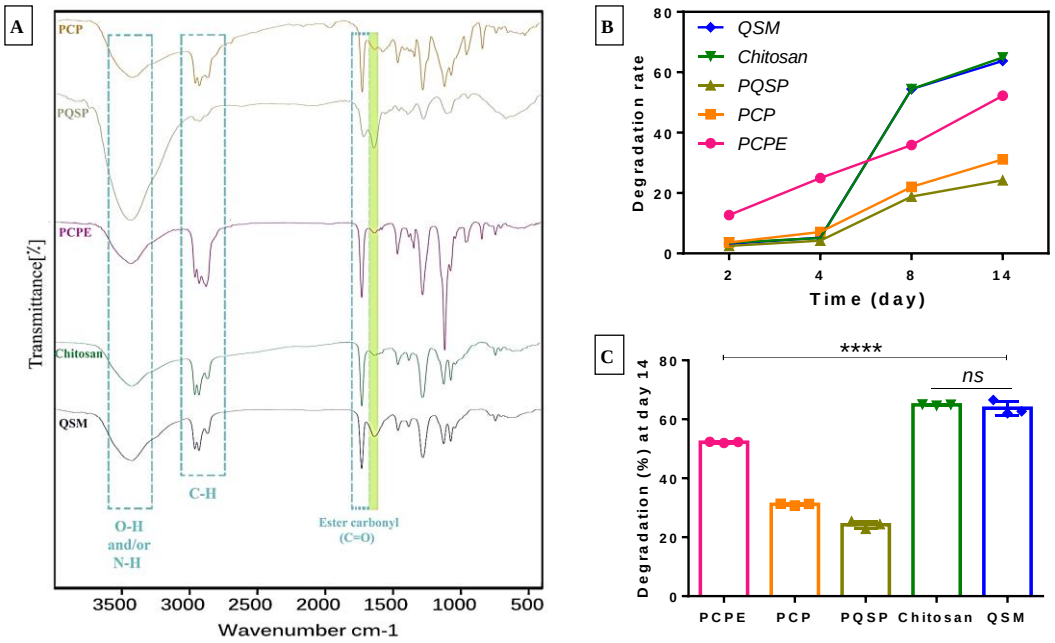

Fig. 1. FTIR spectra (A), the degradation rate during 14 days (B), and the degradation % at day 14 (C). The results are mean ± SD (n=3), ****: p< 0.001 and ns: non-significant difference.

3.2. Degradation rate

The degradation rate of scaffolds plays an important role in the process of tissue regeneration. Some of the tissues such as skin require longer periods of time for the re-epithelialization [1,50]. Thus, the scaffolds that possess more physical stability and strength along with a degradation rate proportional to cells proliferation and differentiation rate can be effective in this field.

As illustrated in Fig. 1B, the degradation rate of all scaffolds increased with time. However, the degradation (%) of the chitosan and QSM scaffolds was much larger relative to other groups, after 14 days (Fig.1C). It can be due to a large number of amine and amide functional

groups in structure of both scaffold that are susceptible to hydrolysis [51]. Furthermore, simple hydrolysis of polymer chains in PCPE scaffold that related to formation of weak intermolecular forces was led to a higher degradation relative to PCP and PQSP hybrid scaffolds ($p< 0.001$). Indeed, the combination of PCPE copolymer with chitosan and QSM was led to ~52% and ~62% decrease in degradation (%) for PCP and PQSP scaffolds, respectively (Fig.1C). It could be due to the more interactions between the polymer chains and formation of stronger chemical bonds between the functional groups of N-H, -OH and C=O.

Hence, it can be deduced that the composite scaffolds based on natural and synthetic polymers can control the degradation % of scaffold and the PCL as an ideal polymer helps to maintain the physical integrity of the scaffold in an aqueous medium due to beter interaction with natural polymers. It was also found that blending a synthetic copolymer with a bioactive material can increase mass remaining of the scaffold and consequently the available surface for cells proliferation and differentiation, composed to natural polymers. Such that, measuring the mass remaining for PCP scaffold, after 14 days exhibited a decrease of approximately 9% compared to the PQSP (Table 1).

In followed by, the swelling assay was carried out to evaluate the absorption capacity of scaffold and to understand how the wound exudates diffuse into the scaffold. Because the swelling capacity of the scaffold (as a wound dressing) is an important factor in exudating wounds [52]. For this purpose, the swelling % was measured after 1 and 24 h of incubation in PBS. The results showed, the swelling % of scaffolds possessed an uptrend during 24 h, except chitosan and QSM scaffolds that can be due to the higher degradation rate (Table 1). The highest swelling percentage was also estimated for PQSP scaffold because of better interactions of QSM hydrophilic groups (amine and hydroxyl) with PCL and PEG, and consequently lower degradation rate, compared to PCP. Thus, the PQSP porous scaffold can be suggested as a 3D wound dressing that enjoy a higher potential in wound exudates absorption, as compared to the chitosan-based scaffold (i.e. PCP).

Table 1. Physicochemical and mechanical parameters of scaffolds

Scaffold code	Mass remaining(%) after 14 days	Swelling (after 1h)	Swelling (after 24h)	Elastic modulus	Tensile strength	Elongation at Break point
PCPE	47.7 ± 0.23	75.4 ± 0.5	187.2 ±1.2	1.4 ± 0.04	2.7 ± 0.22	1.1 ± 0.002[c]
PCP	68.8 ± 0.34	327.4 ± 3.0	394.3 ± 0.3	5.5 ± 0.14[c]	4.4 ± 0.19	1.2 ± 0.004[c]
PQSP	75.7 ± 1.29	373.9 ± 1.6[b]	442.8 ± 1.7	22.8 ± 0.3[d]	13.8 ± 0.58[d]	3.07 ± 0.1[d]
Chitosan	35.1 ± 0.2[a]	365.6 ± 4.8[b]	273.1 ± 2.5[a]	5.1 ± 0.08[a]	1.34 ± 003[a]	0.060 ± 0.0[a]
QSM	36.2 ± 2.43[a]	368.5 ±1.0[b]	278.2 ± 1.6[a]	5.2 ± 0.04[a,c]	1.37 ± 0.03[a]	0.063 ± 0.01[a]

[a]. There is no significant difference between scaffolds ($p> 0.001$).
[b]. There is no significant difference between scaffolds ($p> 0.05$).
[c]. The mean difference is significant at the 0.05 level
[d]. The mean difference is significant at the 0.001 level

3.3. Mechanical behavior analysis

The mechanical characteristics of skin tissue-engineered scaffolds, which are attributed to polymers of scaffold constructor play a crucial role in the promotion of the cellular responses

and cell-scaffold intractions [53]. In this field, some polymers such as PEG can lead to the transduction of mechanical forces (between cells and the surrounding scaffold) into biological signals that results in improvement of cells signaling, prolifferation and differentiation [15,54–56]. However, the combination of polymers can also affect the cells biological behavior via the formation of stronger intermolecular forces, increase/decrease in stiffness and improvement of mechanical resistance of scaffold [17,54]. Therefore, the ideal scaffold should possess suitable biomechanical properties to improve cells behavior (migration, proliferation and differentiation) [15,57].

Here, the mechanical properties of designed scaffolds were evaluated to study the role of polymers in mimicking biomechanical behavior of dermal-ECM. The elastic modulus, tensile strength, and elongation at break point of scaffolds were listed in Table 1.

The results indicate clearly that the mechanical properties of QSM scaffold similar to chitosan ($p>0.05$). This can be explained by the same chemical structures (but different formula). As shown in Fig. 2A, PEPC scaffold indicates the lower elastic modulus than other scaffolds that related to hydrophobic groups of PCL and increase in stiffness of the scaffold structure ($p< 0.001$). The same result was observed in tensile strength and elongation for chitosan and QSM scaffolds that could be due to more hydrophilic groups and an excessive softness of scaffolds structure (Fig. 2B and C, $p<0.001$).

The studies have shown that the balance of stiffness and softness of scaffolds can improve mechanical propertise and regulate the interaction between cell-scaffold [57]. It seems that the combination of natural and synthetic polymers can be effective for this purpose. Our results confirm that adding PCPE copolymer into the chitosan and QSM solutions to make the PCP and PQSP scaffolds, was led to an increase in the mechanical properties due to the existing of the stretching vibrations of hydrogen bonds and carboxylic (O=C-O) groups (Fig. 2.A-C). Although the PQSP scaffold showed better mechanical properties compared to PCP, such that, the modulus, tensile strength, and elongation of PQSP were respectively ~4-fold, 3-fold and 2.5-fold the greater than PCP ($p> 0.001$). This can be due to the different formula of chitosan and QSM that led to the stronger intermolecular forces in the PQSP structure together with the formation of new mini-bands and consequently a balance of stiffness and softness of scaffold. As a consequence, mechanical characteristics of scaffolds based on natural polymer or bioactive material significantly improve, when combined with the synthetic copolymers. Likewise, the comparison of our results with other studies showed that PQSP scaffold is similar, in terms of mechanical function to the decellularized dermal matrix (DDM) and fresh skin [58], although, skin source in the body can affect the modulus [59–61]. However, it is notable that QSM-based scaffold modified by PCPE composite can play an important role in the application of skin tissue engineering.

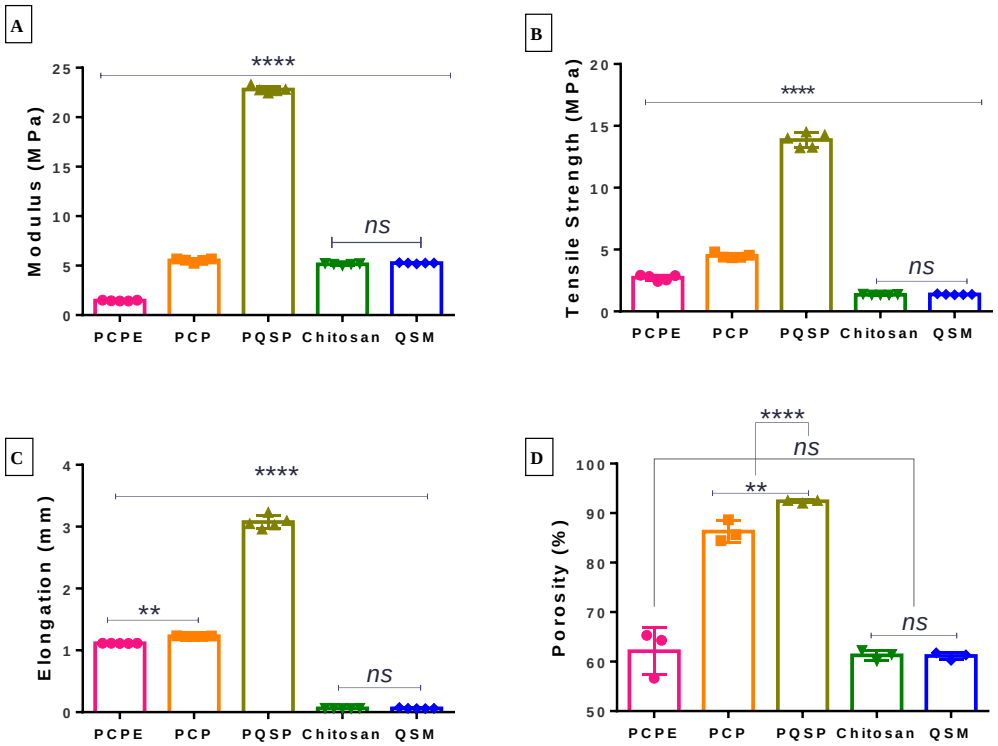

Fig. 2. Mechanical behavior of scafoolds [Modulus (A), Tensile strength (B), and Elongation (C)] along with their porosity % (D). Results are mean ± SD (n=5, 3 respectively), ****: p< 0.001, **: p< 0.05, and ns: non-significant difference.

3.4. Porosity of scaffolds

Based on the reports, the rapid attachment of cells onto the outer edge of the scaffold is the main problem of the using engineered scaffolds in vivo. This process leads to expansion of the necrotic core and consequently the decrease in cell proliferation/differentiation [57]. Therefore, the design of scaffolds with the optimized inner structure that can enhance cells, nutrients and oxygen transfer to the scaffold center will be effective to deal with this issue. The researches in tissue engineering have shown that various materials and methods of scaffolds preparation influence the microstructure of surfaces and consequently cell-scaffold interactions [18,62,63]. Additionally, polymers including functional groups of amine, amide, and hydroxyl lead to the more porosity in scaffold network [57]. Our results confirm the mentioned studies. Table 2 and Figure 2 (D) show the porosity percentage of designed scaffolds. There was no significant difference between QSM, chitosan, and PEPC scaffolds (p> 0.001). It can be explained by weak polymer interactions and/or higher accumulation of functional groups near the wall of the scaffolds. However, the evaluation of porosity % indicated, the combination of natural and synthetic polymers was respectively led to 33% and 28% increase in porosity of PQSP and PCP scaffolds, compared to PCPE (Table 2). The higher porosity was also recorded for PQSP scaffold. The difference in the porosity percentage in the mentioned scaffolds may be caused by a large number of N-H and -OH functional groups that led to an increase in polymer-polymer interactions, mini-bands of inner-network and consequently porosity % of PQSP (p< 0.1).

Table 2. Evaluation and comparison of the physical and structural parameters for all scaffolds

Scaffolds code	Porosity (%)	Mean pore diameters (µm)	Pore diameter range (µm)
PCPE	62.1 ± 4.7 [a]	142.25 ± 4.75	~61-300
PCP	86.2 ± 2.1 [b]	69.67 ± 11.63	~18-90
PQSP	92.3 ± 0.32 [b]	29.27 ± 1.16	~16-57
Chitosan	61.2 ± 1.0 [a]	89.75 ± 2.03	~46-158
QSM	61.1 ± 0.7 [a]	85.3 ± 1.47	~40-145

[a]. There is no significant difference between scaffolds ($p > 0.001$).

[b]. The mean difference is significant at the 0.05 level

3.5. Morphology

SEM images of all scaffolds analyzed to measure pores size and its effect on the cell adhesion and spreading on the surface of scaffold. Figure 3 (A-E) shows the surface morphology of 3D scaffolds.

The results indicated that natural and synthetic polymer-based scaffolds (i.e. QSM, chitosan and PCPE) provided the larger diameter of *pores* that could be due to the limited number of intra- and intermolecular interactions. However, the incorporation of PCPE copolymer with QSM and chitosan was significantly reduced the mean pores diameter of the PQSP and PCP hybrid scaffolds. Although, the smaller pores size was recorded for PQPS scaffold due to better interaction of QSM functional groups with PCPE (Table 2).

The studies have shown that the design of the scaffold with 15-125 µm pores diameter can provide an ideal substrate for differentiation and proliferation of fibroblasts and keratinocytes [57,64]. However, the uniform distribution of pores diameter that results in a more homogenous network can affect initial adhesion and distribution of the cells on the surface of the scaffolds [57,65]. Table 2 and Figure 3 (i-v) indicate the pores diameter range (µm) and diameter distribution histograms, respectively. Here, we found that the higher accumulation of hydroxyl groups in the scaffold network can create the more homogenous 3D-structure along with a large number of pores (higher porosity). This can be explained by the fast freezing of polymeric solutions and then removal of hydroxyl groups from the interstitial spaces of 3D-network, during the freeze-drying process [66]. Thus, PQSP due to presence of the more hydroxyl groups was led to more homogenous structure and uniform distribution of size composed to PCP, chitosan and QSM. On the contrary, the PCPE scaffold showed much larger diameter of pores that attributed to hydrophobic domains in PCL.

As a result, it seems that PQSP scaffold can provide better conditions for enhancing cellular functions (adhesion, proliferation and keratinocyte differentiation) and consequently remodeling dermal-ECM.

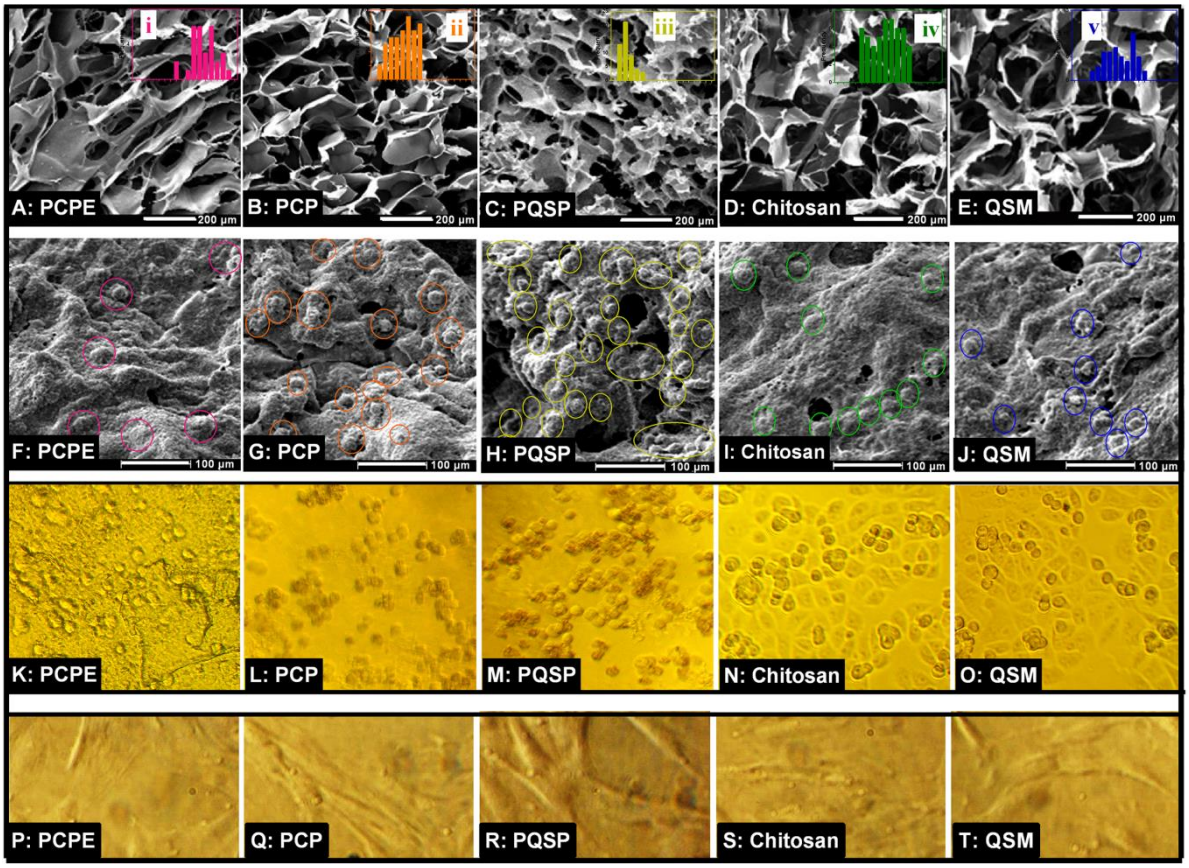

Fig. 3. SEM images of the designed scaffolds before the seeding h-ASCs (A- E), after the seeding h-ASCs (F-J), and the pores diameter distribution histograms (i-v). The inverted microscope images of h-ASCs (K-O) and HSF cells (P-T).

3.6. Cell behavior on the scaffolds

The microstructure of the tissue-engineered scaffolds as 3D-microenvironments provides boundaries for cell growth and differentiation. Morphologically, the ECM-like substrates improve the adhesion of cells and create a more uniform distribution of cell on the surface [18,57,64]. We found that a continuous and interconnected network of scaffold with a porous structure similar to dermal-ECM was dependent on the incorporation of polymers and their source. The bioactive material as higher-quality polymers can play a crucial role in this field.
As Figure 3 (F-J) shows, lowest cell adhesion observed on the synthetic polymer-based scaffold (PCPE) that could be due to the hydrophobic surfaces (chemical properties), formation of simple polymer chains, and larger pores diameter. Based on SEM images, chitosan and QSM scaffolds also presented an almost similar effect on cell adhesion that could be because of the same chemical structures and mechanical properties.

Our results also showed that cells adhesion on the surfaces of chitosan and QSM improved relative to PCPE scaffold, however the cells were sporadically attached to the surfaces. This can be explained by the lack of cell adhesion ligands in the mentioned scaffolds structure.
The various reports have shown that using PEG as a hydrophilic spacer molecule in the scaffold structure can lead to a similar pattern of bioactive compound attachment to the biological surfaces [67,68]. Our study confirms these results. However, we found that PEG can enhance

cell activity when combined with the amide and amine chains of bioactive materials and natural polymers, via electrostatic interactions, the formation of the ligands on the surface, and probably covalent attachment of cell-to-scaffold (Fig. 3F,G and H). Therefore, the presence of PEG in the PCPE structure did not have major impact on the cell attachment process compared to PCP and PQSP. The comparison of SEM images between PCP and PQSP also showed that cellular adhesion and distribution depend on the number and interactions of functional groups. Furthermore, the cells spreading was significantly related to the elastic modulus, porosity (more than 90%) and surface chemistry of substrates (Fig. 3G-H). Hence, more cell adhesion observed for PQSP scaffold.

3.7. cell viability and proliperation

The h-ASCs viability was evaluated by MTT assay (after 24, 48 and 72 h) (Fig. 4). Moreover, proliferation capacity of h-ASCs and HSF cells on scaffolds was determined by inverted microscope images analysis (after 3 days) (Fig. 3K-O and P-T).

As shown in Fig. 4, the h-ASCs viability on scaffolds increased during the 3 days of cell culture, except for chitosan and QSM that can be due to an increase in their degradation rate and lack of physical integrity of the structure and consequently reduction of the surface area available for cell growth. There was significant differences between PCPE and hybrid scaffolds of PCP and PQSP, in terms of cell viability ($p< 0.001$). This can be because of a smaller number of hydrophilic groups in the PEPC structure relative to PCP and PQSP. Because the bioactive compounds such as cells lose their activities, when linked to the scaffolds containing hydrophobic groups [68]. Although, the balance of hydrophilic and hydrophobic groups in the scaffold structure can promote cell proliferation however, evaluation of cell viability showed that there was a significant difference between PCP and PQSP, after 3 days ($p< 0.05$). While, no significant difference was observed between the control group and PQSP, after 48 and 72 h (Fig. 4). This can be due to better physicochemical (porosity, pores size, chemical surface, surface topography, softness/stiffness) and mechanical (elasticity and strength) properties of PQSP relative to PCP that influence cells behaviors (adhesion, viability, prolifaration and differentiation). The inverted microscope images confirmed the data of MTT assay, for all scaffolds (Fig. 3K-O).

As shown in Fig. 3K-T, the PQSP scaffold led to a significant increase in the proliferation of both cells types (h-ASC and HSF cell), compared to other scaffolds. It can be explained by the properties of PQSP scaffold and QSM ability as a bioactive material to stimulate proliferation of fibroblast and stem cells. Therefore, it seems that QSM-based scaffold may contain growth-promoting factors.

The studies have been exhibited that increasing the number of skin cells (such as fibroblasts) on the skin-engineered substrates lead to faster wound healing [69–72]. This point suggests that PQSP can act as a regenerative matrix and potential dressing for the treatment of various wounds and burns.

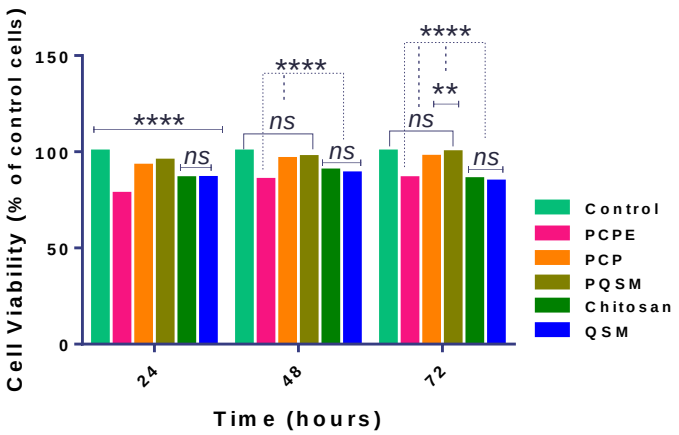

Fig. 4. The h-ASCs viability on scaffolds increased during the 3 days of cell culture. ****: $p< 0.001$, **: $p< 0.05$, and ns: non-significant difference.

3.8. Real-Time PCR and immunocytochemistry analysis

The h-ASCs differentiation capacity into epidermal and dermal keratinocytes (with normal morphology) on scaffolds were assessed by RT-PCR and immunocytochemistry analysis, after 7 and 14 days. As shown in Fig 5A, the K10 and K14 (as early differentiation markers), and K18 (as a late differentiation marker) which are expressed at 3-7 and 14-21 days, respectively [73–75], indicated a higher expression level on PQSP relative to other scaffolds. This could be due to presence of QSM in the mentioned scaffold structure and better interactions of amide and amine chains of this bioactive material with PEG (as a induction factor of biological signals). These factors lead to an increase in crosslinking, elastic modulus and hydrophobicity and consequently can directly affect cellular behavior and growth pattern [8].

Although, the K10 and K14 are known as early markers, the studies of wound healing process have shown that the expression level of K14 on day 3-7 of the skin regeneration process is higher than that of K10. After 7 days, the expression level of both keratinocytes decrease, however K10 indicates a higher expression level compared to K14 [73,76]. This process is related to the mechanism of wound healing and formation of the basal and suprabasal layers, respectively that play an important role in skin regeneration [75].

In this study, the comparison of K14 and K10 expression on the scaffolds (at days 7 and 14) demonstrated that PQSP, QSM, and chitosan scaffolds could imitate such a mechanism. Although, there are significant differences in expression level between PQSP with each of two scaffolds of QSM and chitosan ($p< 0.001$).

According to $2^{-\Delta\Delta Ct}$ method, we did not observe any significant differences in expression levels for K10 and K14 genes between PQSP and TCP (as the control group in epidermal-induction medium) at day 7. In contrast, h-ASCs on PQSP exhibited less K18 induction than TCP (less than 85%), after 14 days. Nonetheless, the gradual induction of this keratinocyte can follow up to 21 days [75].

Furthermore, it was found that chitosan and QSM scaffolds possessed the same function in the induction of keratinocytes differentiation because of similar physicochemical properties. The lower expression level was also observed for these scaffolds (chitosan and QSM) that can be related to weaker 3D-network, physically and mechanically ($p< 0.001$).

It is notable that did not observe any K18 expression on the PCPE scaffold. This can be explained by lack of N-H groups in chemical structure of PCL and PEG. Expression of this keratin is very crucial in the dermal differentiation and re-epithelialization of skin together with its derivative (hair follicles, sebaceous/sweat glands) [75]. Our results showed that the QSM-based hybrid scaffold (PQSP) can be more appropriate candidate for skin tissue engineering applications composed to chitosan-based hybrid scaffolds (PCP) and can function as an induction substrate or wound dressing.

Based on the results of RT-PCR, the immunocytochemical study was performed for only two groups of PCP and PQSP due to the better results of keratinocytes differentiation. Three types of antibodies were used to detect epidermal and dermal markers expressed at two different differentiation stages: keratins 10 and 14 (early) as epidermal keratinocytes and keratins 18 (late) as dermal keratinocytes. The expression and morphology of K10, K14, and K18 were observed after 7 and 14 days of cell culture on PCP and PQSP. As illustrated in Fig 5B, the distinguishable phenotypical feature of epidermal and dermal keratinocytes are observed on each of the two scaffolds. The h-ASCs which grown on two scaffolds exhibited polygonal and round morphologies. However, PQSP led to a significant increase in keratinocytes induction and proliferation, in the absence of growth factor, compared to PCP. Such that, the K10, K14, and K18 expression on the PQSP were respectively recorded ~1.5, 2 and 1.6-fold the higher than PCP, after 7 and 14 days (Fig. 5A). This can be due to the existing of various functional groups in the PQSP structure than PCP. Surface chemitry assay (FTIR) confirms this result.
Overall, the results of RT-PCR and immunocytochemistry analysis indicated that novel 3D PQSP scaffold can induct both epidermal and dermal keratinocytes by h-ASCs differentiation (in a desirable level for wound healing), via mimicking the structure and function of dermal-ECM and increasing the mechanical signals transduction into the biological signals that result in the imitative of the normal phenotype and differentiation pattern of epidermal and dermal cells (in the early and late phases). These features are owing to the existence of QSM bioactive material in the structure of PQSP scaffold.

This preliminary study suggests that QSM can function as an important factor in skin tissue engineering for induction of keratinocytes, acceleration of cells growth and wound healing.

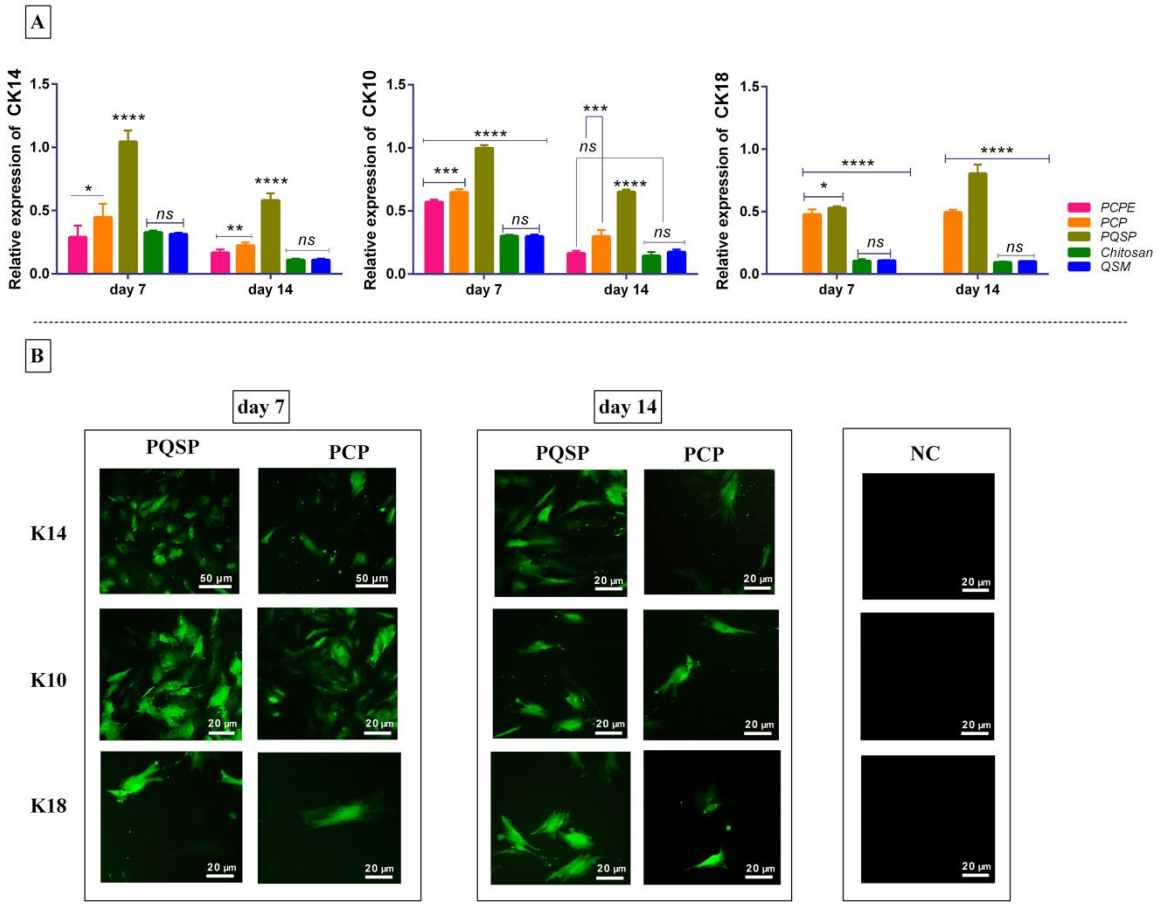

Fig. 5. Expression of K14, K10, and K18 on all five scaffolds (A) along with immunecytochemical analysis for the expression of the mentioned keratinocytes on only PQSP and PCP scaffolds (B), at days 7 and 14. Results are mean ± SD (n=3). ****: p< 0.001, ***: p< 0.01, **: p< 0.05, *: p< 0.1, ns: non-significant difference, and NC: negative control.

Conclusion

In the present study, a novel hybrid scaffold (PQSP) containing quince seed mucilage and PCL-PEG composite was designed to achieve an ideal substrate for skin tissue engineering applications. Four other scaffolds based on natural and synthetic polymers (PCPE, PCP, chitosan, and quince-seed mucilage (QSM)) were also fabricated to determine the role of extracted mucilage (gel) from quince-seeds in improving physicochemical, biomechanical and structural properties of scaffold, and to understand the cellular behavior on the engineeried substrates. Our results suggested that PQSP hybrid scaffold can support human dermal fibroblasts proliferation via providing a porous network with the appropriate pores size for the growth of skin cells. Moreover, the high water absorption capacity of this scaffold compared to other scaffolds showed that can act as a suitable dressing for continuous absorption of wound exudates. We also have demonstrated, for the first time, that the QSM, when were combined with PEG, can be more effective than that of chitosan, in terms of mechanical force-induced signals transduction (mechanical force between cell and scaffold) into the biological signals and induction of h-ASC differentiation into both keratinocytes of dermal and epidermal. Furthermore, it was found that the presence of QSM in the hybrid scaffold structure can create

not only proper factors to promote cell proliferation and differentiation but also provide a differentiation pattern similar to epidermis and dermis keratinocytes. Thus, QSM as a differentiation-promoting factor (smart biomaterial) and inexpensive material can be effective to integrate into skin tissue-engineered scaffolds and develop smart/stimuli-responsive bio-matrix (wound dressings or scaffolds containing cells, growth factor-free). In our opinion, this study can provide new insight into the design of dermal ECM-like 3D-microenvironment, based on bioactive materials/molecules, and sheds light on the therapeutic applications of such scaffolds.

Conflicts of interest

The authors declare that they have no competing interests.

Formatting of funding sources

This research did not receive any specific grant from funding agencies in the public, commercial, or not-for-profit sectors.

Acknowledgments

Authors would like to express our deep appreciation to Dr. Arash Sarveazad for his scientific guidance, and encouragement throughout this project.

Reference

[1] L. Rittié, Cellular mechanisms of skin repair in humans and other mammals, J. Cell Commun. Signal. 10 (2016) 103–120. doi:10.1007/s12079-016-0330-1.

[2] M. Geerligs, Skin layer mechanics, Ski. Layer Mech. (2009) 122.

[3] M. Varkey, J. Ding, E. Tredget, Advances in Skin Substitutes—Potential of Tissue Engineered Skin for Facilitating Anti-Fibrotic Healing, J. Funct. Biomater. 6 (2015) 547–563. doi:10.3390/jfb6030547.

[4] A.C.H.R. Machado, P.S. Lopes, C.P. Raffier, I.N. Haridass, M. Roberts, J. Grice, V.R. Leite-Silva, Skin Penetration, in: Cosmet. Sci. Technol. Theor. Princ. Appl., Elsevier Inc., 2017: pp. 741–755. doi:10.1016/B978-0-12-802005-0.00046-X.

[5] B.K. Sun, Z. Siprashvili, P.A. Khavari, Advances in skin grafting and treatment of cutaneous wounds, Science (80-.). 346 (2014) 941–945. doi:10.1126/science.1253836.

[6] X. Wang, C. You, X. Hu, Y. Zheng, Q. Li, Z. Feng, H. Sun, C. Gao, C. Han, The roles of knitted mesh-reinforced collagen-chitosan hybrid scaffold in the one-step repair of full-thickness skin defects in rats, Acta Biomater. 9 (2013) 7822–7832. doi:10.1016/j.actbio.2013.04.017.

[7] S. Kellouche, C. Martin, G. Korb, R. Rezzonico, D. Bouard, M. Benbunan, L. Dubertret, C. Soler, C. Legrand, C. Dosquet, Tissue engineering for full-thickness burns: A dermal substitute from bench to bedside, Biochem. Biophys. Res. Commun. 363 (2007) 472–478. doi:10.1016/j.bbrc.2007.08.155.

[8] Y. Pilehvar-Soltanahmadi, M. Nouri, M.M. Martino, A. Fattahi, E. Alizadeh, M. Darabi, M. Rahmati-Yamchi, N. Zarghami, Cytoprotection, proliferation and epidermal differentiation of adipose tissue-derived stem cells on emu oil based electrospun nanofibrous mat, Exp. Cell Res. 357 (2017) 192–201. doi:10.1016/j.yexcr.2017.05.015.

[9] S.P. Zhong, Y.Z. Zhang, C.T. Lim, Tissue scaffolds for skin wound healing and dermal

reconstruction, Wiley Interdiscip. Rev. Nanomedicine Nanobiotechnology. 2 (2010) 510–525. doi:10.1002/wnan.100.
[10] Y. Wu, Y. Han, 3D functional scaffolds for tendon tissue engineering, in: Funct. 3D Tissue Eng. Scaffolds, Elsevier, 2017: pp. 367–390. doi:10.1016/b978-0-08-100979-6.00015-x.
[11] Zhang, Duan, Feng, Guo, Wang, Zhao, Zhou, Wei, Cao, Engineering of epidermis skin grafts using electrospun nanofibrous gelatin/polycaprolactone membranes, Int. J. Nanomedicine. (2013) 2077. doi:10.2147/IJN.S42384.
[12] S. Miguel, M. Ribeiro, P. Coutinho, I. Correia, Electrospun Polycaprolactone/Aloe Vera_Chitosan Nanofibrous Asymmetric Membranes Aimed for Wound Healing Applications, Polymers (Basel). 9 (2017) 183. doi:10.3390/polym9050183.
[13] S.S. Silva, E.G. Popa, M.E. Gomes, M. Cerqueira, A.P. Marques, S.G. Caridade, P. Teixeira, C. Sousa, J.F. Mano, R.L. Reis, An investigation of the potential application of chitosan/aloe-based membranes for regenerative medicine, Acta Biomater. 9 (2013) 6790–6797. doi:10.1016/j.actbio.2013.02.027.
[14] B. Dash, Z. Xu, L. Lin, A. Koo, S. Ndon, F. Berthiaume, A. Dardik, H. Hsia, Stem Cells and Engineered Scaffolds for Regenerative Wound Healing, Bioengineering. 5 (2018) 23. doi:10.3390/bioengineering5010023.
[15] A. A. Chaudhari, K. Vig, D. [Radé Baganizi, R. Sahu, S. Dixit, V. Dennis, S. Ram Singh, S. R. Pillai, Future Prospects for Scaffolding Methods and Biomaterials in Skin Tissue Engineering: A Review, Int. J. Mol. Sci. 17 (2016) 1974. doi:10.3390/ijms17121974.
[16] E.J. Chong, T.T. Phan, I.J. Lim, Y.Z. Zhang, B.H. Bay, S. Ramakrishna, C.T. Lim, Evaluation of electrospun PCL/gelatin nanofibrous scaffold for wound healing and layered dermal reconstitution, Acta Biomater. 3 (2007) 321–330. doi:10.1016/j.actbio.2007.01.002.
[17] F.J. O'Brien, Biomaterials & scaffolds for tissue engineering, Mater. Today. 14 (2011) 88–95. doi:10.1016/S1369-7021(11)70058-X.
[18] L. Ghasemi-Mobarakeh, Structural properties of scaffolds: Crucial parameters towards stem cells differentiation, World J. Stem Cells. 7 (2015) 728. doi:10.4252/wjsc.v7.i4.728.
[19] A. Asif, G. Kakub, S. Mehmood, R. Khunum, M. Gulfraz, Wound healing activity of root extracts ofBerberis lyceum royle in rats, Phyther. Res. 21 (2007) 589–591. doi:10.1002/ptr.2110.
[20] A.A. Hemmati, F. Mohammadian, An Investigation into the Effects of Mucilage of Quince Seeds on Wound Healing in Rabbit, J. Herbs. Spices Med. Plants. 7 (2000) 41–46. doi:10.1300/J044v07n04_05.
[21] Subashini. S, K.D. Arunachalam, S.K. Annamalai, Preclinical studies on the phytochemical, antimicrobial, and wound healing properties of indigofera aspalathoides leaves, J. Pharm. Res. 4 (2011) 3206–3211.
[22] K.D. Arunachalam, S. Subhashini, Investigations on the phytochemical activities and wound healing properties of Adhatoda vasica leave in Swiss albino mice, African J. Plant Sci. 5 (2011) 133–145. http://www.academicjournals.org/ajps.
[23] M. Liu, Y. Dai, Y. Li, Y. Luo, F. Huang, Z. Gong, Q. Meng, Madecassoside isolated from Centella asiatica herbs facilitates burn wound healing in mice, Planta Med. 74 (2008) 809–815. doi:10.1055/s-2008-1074533.
[24] M. Afshar, R. Ghaderi, M. Zardast, P. Delshad, Effects of Topical Emu Oil on Burn Wounds in the Skin of Balb/c Mice., Dermatol. Res. Pract. 2016 (2016) 6419216. doi:10.1155/2016/6419216.
[25] M. Fronza, B. Heinzmann, M. Hamburger, S. Laufer, I. Merfort, Determination of the wound healing effect of Calendula extracts using the scratch assay with 3T3 fibroblasts., J. Ethnopharmacol. 126 (2009) 463–467. doi:10.1016/j.jep.2009.09.014.
[26] G. Dixit, G. Misal, V. Gulkari, K. Upadhye, FORMULATION AND EVALUATION OF POLYHERBAL GEL FOR ANTI - INFLAMMATORY ACTIVITY Gouri, Int. J. Pharm. Sci. Res. 4 (2013) 1186–1191. doi:10.13040/IJPSR.0975-8232.4(3).1186-91.
[27] F.A. Toppo, R.S. Pawar, Development, optimization and evaluation of different herbal formulations for wound healing, Int. J. Pharm. Pharm. Sci. 7 (2015) 447–452.
[28] S. Fahimi, S.A. Mortazavi, M. Abdollahi, H. Hajimehdipoor, Formulation of a traditionally used polyherbal product for burn healing and HPTLC fingerprinting of its phenolic contents, Iran. J. Pharm. Res. 15 (2016) 95–105.

[29] S. Vamsi, C. Satish, K. Nagaveni, J.M. Joy, P. Latha, Formulation and Evaluation of Polyherbal Wound Healing Ointment, Intl. R. J. Pharm. 3 (2014) 66–73.
[30] A.I. Aghmiuni, A.A. Khiavi, Medicinal Plants to Calm and Treat Psoriasis Disease, in: H.A. El-Shemy (Ed.), Aromat. Med. Plants - Back to Nat., InTech, Rijeka, 2017: pp. 1–28. doi:10.5772/67062.
[31] G. Jin, M.P. Prabhakaran, D. Kai, S.K. Annamalai, K.D. Arunachalam, S. Ramakrishna, Tissue engineered plant extracts as nanofibrous wound dressing, Biomaterials. 34 (2013) 724–734. doi:10.1016/j.biomaterials.2012.10.026.
[32] M. Ghafourian, P. Tamri, A. Hemmati, Enhancement of Human Skin Fibroblasts Proliferation as a Result of Treating With Quince Seed Mucilage, Jundishapur J. Nat. Pharm. Prod. 10 (2015) 10–13. doi:10.17795/jjnpp-18820.
[33] S. Soumya, K.M. Sajesh, R. Jayakumar, S. V. Nair, K.P. Chennazhi, Development of a phytochemical scaffold for bone tissue engineering using Cissus quadrangularis extract, Carbohydr. Polym. 87 (2012) 1787–1795. doi:10.1016/j.carbpol.2011.09.094.
[34] Y. Pilehvar-Soltanahmadi, M. Dadashpour, A. Mohajeri, A. Fattahi, R. Sheervalilou, N. Zarghami, An Overview on Application of Natural Substances Incorporated with Electrospun Nanofibrous Scaffolds to Development of Innovative Wound Dressings., Mini Rev. Med. Chem. 18 (2018) 414–427. doi:10.2174/1389557517666170308112147.
[35] A.A. Hemmati, H. Kalantari, A. Jalali, S. Rezai, H.H. Zadeh, Healing effect of quince seed mucilage on T-2 toxin-induced dermal toxicity in rabbit, Exp. Toxicol. Pathol. 64 (2012) 181–186. doi:10.1016/j.etp.2010.08.004.
[36] J.-M. Wang, Y. Gu, C.-J. Pan, L.-R. Yin, Isolation, culture and identification of human adipose-derived stem cells, Exp. Ther. Med. 13 (2017) 1039–1043. doi:10.3892/etm.2017.4069.
[37] P. Palumbo, F. Lombardi, G. Siragusa, M. Cifone, B. Cinque, M. Giuliani, Methods of Isolation, Characterization and Expansion of Human Adipose-Derived Stem Cells (ASCs): An Overview, Int. J. Mol. Sci. 19 (2018) 1897. doi:10.3390/ijms19071897.
[38] X. Zhao, X. Sun, L. Yildirimer, Q. Lang, Z.Y. (William) Lin, R. Zheng, Y. Zhang, W. Cui, N. Annabi, A. Khademhosseini, Cell infiltrative hydrogel fibrous scaffolds for accelerated wound healing, Acta Biomater. 49 (2017) 66–77. doi:10.1016/j.actbio.2016.11.017.
[39] Q. Tan, S. Li, J. Ren, C. Chen, Fabrication of Porous Scaffolds with a Controllable Microstructure and Mechanical Properties by Porogen Fusion Technique, Int. J. Mol. Sci. 12 (2011) 890–904. doi:10.3390/ijms12020890.
[40] ASTM D3039/D3039M-00 “Standard Test Method for Tensile Properties of Polymer Matrix Composite Materials” DOI: 10.1520/D3039_D3039M-00, (n.d.). https://www.astm.org/DATABASE.CART/HISTORICAL/D3039D3039M-00.htm (accessed March 12, 2019).
[41] B.P. Antunes, A.F. Moreira, V.M. Gaspar, I.J. Correia, Chitosan/arginine–chitosan polymer blends for assembly of nanofibrous membranes for wound regeneration, Carbohydr. Polym. 130 (2015) 104–112. doi:10.1016/j.carbpol.2015.04.072.
[42] S. Heidari Keshel, M. Rostampour, G. Khosropour, A. Bandbon B, A. Baradaran-Rafii, E. Biazar, Derivation of epithelial-like cells from eyelid fat-derived stem cells in thermosensitive hydrogel, J. Biomater. Sci. Polym. Ed. 27 (2015) 339–350. doi:10.1080/09205063.2015.1130406.
[43] N. Düzgüneş, C.T. De Ilarduya, Genetic nanomedicine: Gene delivery by targeted lipoplexes, Methods Enzymol. 509 (2012) 355–367. doi:10.1016/B978-0-12-391858-1.00018-6.
[44] S.S. Sarvandi, M.T. Joghataei, K. Parivar, M. Khosravi, A. Sarveazad, N. Sanadgol, In vitro differentiation of rat mesenchymal stem cells to hepatocyte lineage, Iran. J. Basic Med. Sci. 18 (2015) 89–97.
[45] M.A. Hussain, G. Muhammad, M.T. Haseeb, M.N. Tahir, Quince Seed Mucilage: A Stimuli-Responsive/Smart Biopolymer, in: M.A. Jafar Mazumder, H. Sheardown, A. Al-Ahmed (Eds.), Funct. Biopolym., Springer International Publishing, Cham, 2019: pp. 127–148. doi:10.1007/978-3-319-95990-0_19.
[46] F.J. O’Brien, B.A. Harley, I.V. Yannas, L.J. Gibson, The effect of pore size on cell adhesion in collagen-GAG scaffolds, Biomaterials. 26 (2005) 433–441. doi:10.1016/j.biomaterials.2004.02.052.

[47] A.J. Engler, S. Sen, H.L. Sweeney, D.E. Discher, Matrix Elasticity Directs Stem Cell Lineage Specification, Cell. 126 (2006) 677–689. doi:10.1016/j.cell.2006.06.044.
[48] S.R. Peyton, A.J. Putnam, Extracellular matrix rigidity governs smooth muscle cell motility in a biphasic fashion, J. Cell. Physiol. 204 (2005) 198–209. doi:10.1002/jcp.20274.
[49] J. Coates, Interpretation of Infrared Spectra, A Practical Approach, in: Encycl. Anal. Chem., John Wiley & Sons, Ltd, Chichester, UK, 2006: pp. 1–23. doi:10.1002/9780470027318.a5606.
[50] V.T. Nguyen, N. Farman, E. Maubec, D. Nassar, D. Desposito, L. Waeckel, S. Aractingi, F. Jaisser, Re-Epithelialization of Pathological Cutaneous Wounds Is Improved by Local Mineralocorticoid Receptor Antagonism, J. Invest. Dermatol. 136 (2016) 2080–2089. doi:10.1016/j.jid.2016.05.101.
[51] T. Snape, Astles.Alison, J. Davies, A. Astles, J. Davies, Understanding the chemical basis of drug stability and degradation, Pharm. J. 385 (2010) 416–417. http://www.pharmaceutical-journal.com/opinion/comment/understanding-the-chemical-basis-of-drug-stability-and-degradation/11029512.article.
[52] R.F. El-Kased, R.I. Amer, D. Attia, M.M. Elmazar, Honey-based hydrogel: In vitro and comparative In vivo evaluation for burn wound healing, Sci. Rep. 7 (2017) 9692. doi:10.1038/s41598-017-08771-8.
[53] B.P. Chan, K.W. Leong, Scaffolding in tissue engineering: general approaches and tissue-specific considerations, Eur. Spine J. 17 (2008) 467–479. doi:10.1007/s00586-008-0745-3.
[54] Y. Javadzadeh, S. Hamedeyaz, Floating Drug Delivery Systems for Eradication of Helicobacter pylori in Treatment of Peptic Ulcer Disease, in: Trends Helicobacter Pylori Infect., InTech, 2014: p. 13. doi:10.5772/57353.
[55] K.I. Shingel, L. Di Stabile, J.-P. Marty, M.-P. Faure, Inflammatory inert poly(ethylene glycol)?protein wound dressing improves healing responses in partial- and full-thickness wounds, Int. Wound J. 3 (2006) 332–342. doi:10.1111/j.1742-481X.2006.00262.x.
[56] P. Vermette, L. Meagher, Interactions of phospholipid- and poly(ethylene glycol)-modified surfaces with biological systems: relation to physico-chemical properties and mechanisms, Colloids Surfaces B Biointerfaces. 28 (2003) 153–198. doi:10.1016/S0927-7765(02)00160-1.
[57] H.-I. Chang, Y. Wang, Cell Responses to Surface and Architecture of Tissue Engineering Scaffolds, in: Regen. Med. Tissue Eng. - Cells Biomater., InTech, 2011: p. 64. doi:10.5772/21983.
[58] P.B. Milan, N. Lotfibakhshaiesh, M.T. Joghataie, J. Ai, A. Pazouki, D.L. Kaplan, S. Kargozar, N. Amini, M.R. Hamblin, M. Mozafari, A. Samadikuchaksaraei, Accelerated wound healing in a diabetic rat model using decellularized dermal matrix and human umbilical cord perivascular cells., Acta Biomater. 45 (2016) 234–246. doi:10.1016/j.actbio.2016.08.053.
[59] A. Karimi, M. Haghighatnama, A. Shojaei, M. Navidbakhsh, A. Motevalli Haghi, S.J. Adnani Sadati, Measurement of the viscoelastic mechanical properties of the skin tissue under uniaxial loading, Proc. Inst. Mech. Eng. Part L J. Mater. Des. Appl. 230 (2016) 418–425. doi:10.1177/1464420715575169.
[60] T.M. MacLeod, A. Cambrey, G. Williams, R. Sanders, C.J. Green, Evaluation of Permacol as a cultured skin equivalent., Burns. 34 (2008) 1169–1175. doi:10.1016/j.burns.2008.01.013.
[61] M. Vitacolonna, M. Mularczyk, F. Herrle, T.J. Schulze, H. Haupt, M. Oechsner, L.R. Pilz, P. Hohenberger, E.D. Rössner, Effect on the tensile strength of human acellular dermis (Epiflex®) of in-vitro incubation simulating an open abdomen setting, BMC Surg. 14 (2014) 7. doi:10.1186/1471-2482-14-7.
[62] M. Wang, X. Cheng, W. Zhu, B. Holmes, M. Keidar, L.G. Zhang, Design of Biomimetic and Bioactive Cold Plasma-Modified Nanostructured Scaffolds for Enhanced Osteogenic Differentiation of Bone Marrow-Derived Mesenchymal Stem Cells, Tissue Eng. Part A. 20 (2014) 1060–1071. doi:10.1089/ten.tea.2013.0235.
[63] F. Pan, M. Zhang, G. Wu, Y. Lai, B. Greber, H.R. Schöler, L. Chi, Topographic effect on human induced pluripotent stem cells differentiation towards neuronal lineage, Biomaterials. 34 (2013) 8131–8139. doi:10.1016/j.biomaterials.2013.07.025.
[64] Q.L. Loh, C. Choong, Three-Dimensional Scaffolds for Tissue Engineering Applications: Role of Porosity and Pore Size, Tissue Eng. Part B Rev. 19 (2013) 485–502. doi:10.1089/ten.teb.2012.0437.

[65] C.M. Murphy, F.J. O'Brien, Understanding the effect of mean pore size on cell activity in collagen-glycosaminoglycan scaffolds, Cell Adh. Migr. 4 (2010) 377–381. doi:10.4161/cam.4.3.11747.
[66] Z. Fereshteh, Freeze-drying technologies for 3D scaffold engineering, in: Y. Deng, J. Kuiper (Eds.), Funct. 3D Tissue Eng. Scaffolds, Elsevier, 2018: pp. 151–174. doi:10.1016/B978-0-08-100979-6.00007-0.
[67] D.A. Puleo, R. Bizios, Biological Interactions on Materials Surfaces: Understanding and Controlling Protein, Cell, and Tissue Responses, Springer New York, 2009. https://books.google.com/books?id=XU4ofeKjfQ4C.
[68] J.M. Goddard, J.H. Hotchkiss, Polymer surface modification for the attachment of bioactive compounds, Prog. Polym. Sci. 32 (2007) 698–725. doi:10.1016/j.progpolymsci.2007.04.002.
[69] K. Vig, A. Chaudhari, S. Tripathi, S. Dixit, R. Sahu, S. Pillai, V. Dennis, S. Singh, Advances in Skin Regeneration Using Tissue Engineering, Int. J. Mol. Sci. 18 (2017) 789. doi:10.3390/ijms18040789.
[70] Y. Liu, H. Luo, X. Wang, A. Takemura, Y.R. Fang, Y. Jin, F. Suwa, In Vitro Construction of Scaffold-Free Bilayered Tissue-Engineered Skin Containing Capillary Networks, Biomed Res. Int. 2013 (2013) 1–8. doi:10.1155/2013/561410.
[71] K. Boehnke, N. Mirancea, A. Pavesio, N.E. Fusenig, P. Boukamp, H.-J. Stark, Effects of fibroblasts and microenvironment on epidermal regeneration and tissue function in long-term skin equivalents, Eur. J. Cell Biol. 86 (2007) 731–746. doi:10.1016/j.ejcb.2006.12.005.
[72] Y. Wu, L. Chen, P.G. Scott, E.E. Tredget, Mesenchymal Stem Cells Enhance Wound Healing Through Differentiation and Angiogenesis, Stem Cells. 25 (2007) 2648–2659. doi:10.1634/stemcells.2007-0226.
[73] E. Lane, W. McLean, Keratins and skin disorders, J. Pathol. 204 (2004) 355–366. doi:10.1002/path.1643.
[74] A. Webb, A. Li, P. Kaur, Location and phenotype of human adult keratinocyte stem cells of the skin, Differentiation. 72 (2004) 387–395. doi:10.1111/j.1432-0436.2004.07208005.x.
[75] L. Zhang, Keratins in Skin Epidermal Development and Diseases, in: Keratin, IntechOpen, 2018: p. 13. doi:10.5772/intechopen.79050.
[76] H. Alam, L. Sehgal, S.T. Kundu, S.N. Dalal, M.M. Vaidya, Novel function of keratins 5 and 14 in proliferation and differentiation of stratified epithelial cells, Mol. Biol. Cell. 22 (2011) 4068–4078. doi:10.1091/mbc.e10-08-0703.